Hindawi
Geofluids
Volume 2022, Article ID 4679547, 14 pages
https://doi.org/10.1155/2022/4679547

Research Article

Experimental Study on the Effect of Initial Water Content and Temperature Gradient on Soil Column Segregation Frost Heave

Dong Zhang,[1] **Meng Wang**,[1,2] **Xiao-kang Li**,[1] **and A-qiang Liu**[1]

[1]*School of Civil Engineering, Beijing Jiaotong University, Beijing 100044, China*
[2]*Shijiazhuang Tiedao University, Shijiazhuang, Hebei 050043, China*

Correspondence should be addressed to Dong Zhang; 18115056@bjtu.edu.cn

Received 7 August 2022; Revised 13 September 2022; Accepted 20 September 2022; Published 8 October 2022

Academic Editor: Dongdong Ma

A series of freezing experiments were carried out on the Qinghai silty clay using a one-dimensional soil column particle image velocimetry (PIV) system. The effects of the initial water content and temperature gradient on the frost heave of the soil column were analysed. The experimental results show that the total volumetric water content after the Qinghai silty clay freezing is much greater than the initial water content before freezing, and the total volumetric water content at the segregated layer reaches the maximum value. The average unfrozen water content firstly increases sharply with time and then decreases slowly. The obvious horizontal layered segregation cracks filled with unsaturated needle-columnar ice lenses have occurred above the soil column frozen fringe. The thickness of segregated ice is about 43% of the total frost heave. There is a small frost heave in the frozen fringe and a small compression deformation amount in the unfrozen zone. Under the same temperature gradient conditions, the soil column with the low initial water content has a smaller frozen depth, larger total volumetric water content, more water intake, smaller segregated ice thickness, and less total frost heave amount than that of the soil column with the high initial water content. Under the same initial water content conditions, the soil column with a large temperature gradient has a greater frozen depth, consistent total volumetric water content, larger segregated ice thickness, and greater total frost heave amount than that of the soil column with a small temperature gradient.

1. Introduction

When the soil temperature is lower than the freezing temperature of the water in the soil, the liquid water in the soil usually undergoes a phase change and condenses into an ice lens. The formation of segregated ice will result in a large amount of frost heave in the soil, which will bring diseases to the cold area projects, such as the deformation of subgrade frost heave [1–5] and the frost heave cracking of channel lining [6, 7]. Frost heave is one of the main frost damages in geotechnical engineering in cold regions [8]. Therefore, the experimental research on the soil segregation frost heave provides a reference for the theory and test of frozen soil.

A lot of research has been done on the problem of soil frost heave. Konrad et al. [9] studied the water migration test during the freezing process of saturated fine-grained soil under an open system and proposed the theory of segregation potential. Xu et al. [10] discussed several types of frost heave development of saturated soil under an open system and proposed the formula for predicting frost heave by using field temperature gradient. Zhao et al. [11] studied the effect of initial moisture content and temperature on water migration during the freezing process of undisturbed silty clay under a closed system. Wei et al. [12] studied the influence of the boundary temperature and soil sample height on water migration during the freezing process of saturated silt under an open system. Liu et al. [13] studied the three-dimensional isothermal volume change of unsaturated soil under different saturation and initial void ratio in a closed system. Wang et al. [14] revealed the cryogenic structure and frost heave deformation law of frozen soil by one-dimensional freezing test of the saturated Qinghai-Tibet silty clay under an open system. Huang [15] found that the frost heave amount of soil sample increases with the initial degree of saturation through the unit freezing test of unsaturated soil under a closed system when the degree of compaction

Table 1: The basic physical parameters of the Qinghai silty clay.

Maximum dry density ($g{\cdot}cm^{-3}$)	Optimal water content (%)	Liquid limit (%)	Plastic limit (%)	Plasticity index	Specific gravity	Specific surface area ($m^2{\cdot}g^{-1}$)
1.746	15.20	26.75	14.31	12.44	2.73	17.62

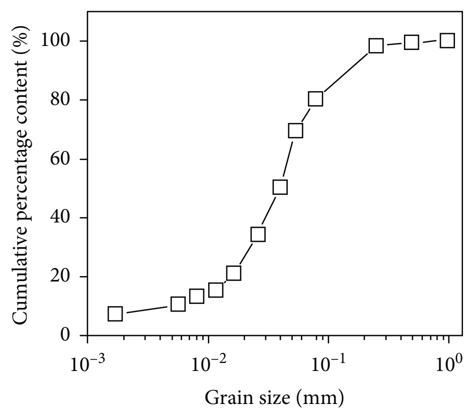

Figure 1: The particle gradation curve of the Qinghai silty clay.

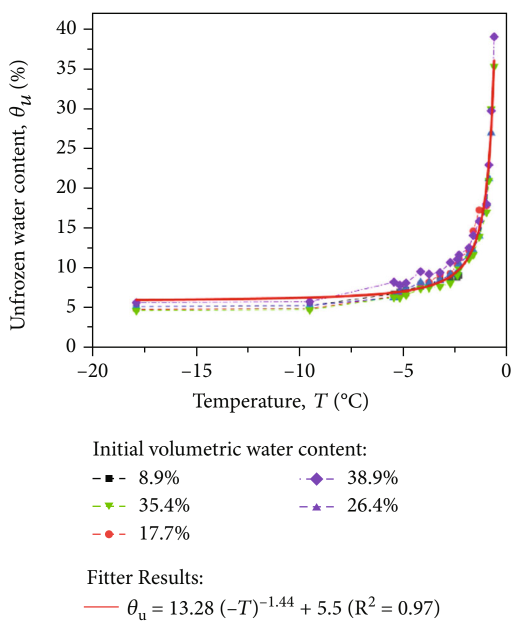

Figure 2: The soil freezing characteristic curve (SFCC) of the Qinghai silty clay.

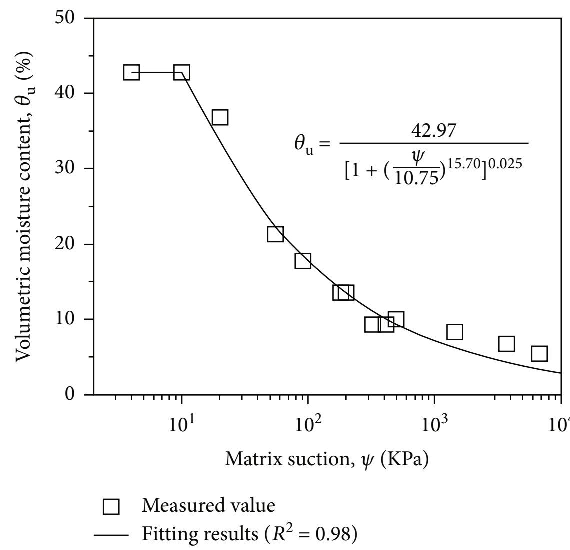

Figure 3: The soil-water characteristic curve (SWCC) of the Qinghai silty clay.

is constant. Ren et al. [16] conducted unidirectional freezing experiments on the effects of initial water content, freeze-thaw times, and freezing temperature on the frost heave characteristics of clay under a closed system and found that the initial water content had the greatest impact on segregated ice. Xiao et al. [17] studied the law and mechanism of water and salt migration during the freezing process of saline soil. However, these studies did not consider the freezing of unsaturated soil or the water replenishment under an open system and cannot quantitatively measure the local deformation of frozen soil, which had certain limitations for further exploring the law of frost heave. Go et al. and Jin et al. [18, 19] studied the effect of temperature boundary conditions, porosity, and height of the specimen on the sandy soil frost heave by one-dimensional frost heave test and numerical simulation. Wang et al. [20] developed a frozen soil test system based on digital image technology, which can be used to observe the cryogenic structure and ice segregation process and measure frost heave deformation during freezing. But the system cannot be used to continuously measure the local strain field of frozen soil quantitatively. Zhou and Zhang [21] developed a new type of visual freeze-thaw test system. It can be used to automatically control the temperature state of the soil and observe the development state of the segregated ice during the frost heave. However, it also cannot be calculated the local deformation of the frozen soil.

To sum up, to solve the problems that it is difficult to observe the morphological characteristics of segregated ice and quantitatively measure the thickness of segregated ice and the local strain in the segregation zone in the traditional one-dimensional soil column freezing test, a one-dimensional soil column particle image velocimetry (PIV) digital freezing test system was developed. Meanwhile, a series of freezing tests on the Qinghai silty clay under an open system was carried out to analyse the effects of different initial water contents and temperature gradients on the soil column frost heave. Local deformation and strain of soil column under different freezing conditions were measured

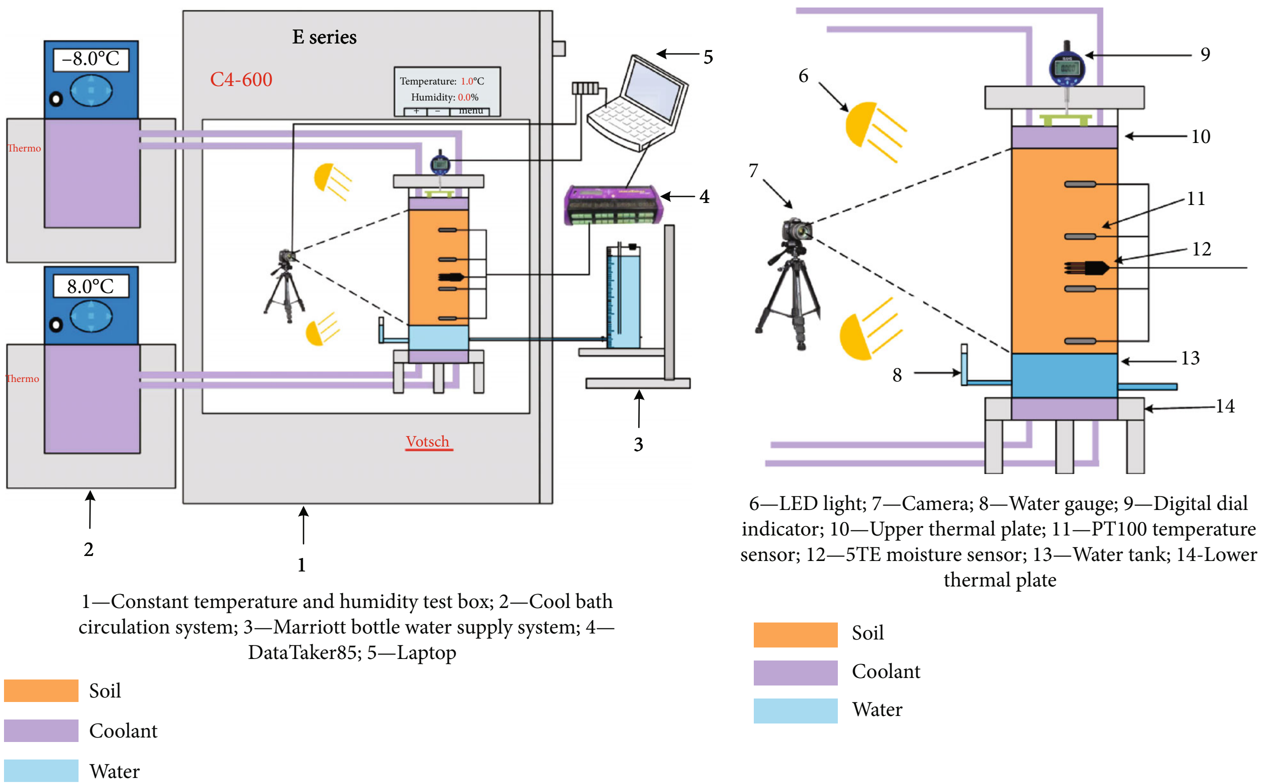

(a) Overall schematic

(b) The soil column cylinder system schematic

Figure 4: The experiment system composition schematic.

Table 2: The soil column frost heave test scheme.

Soil column	Cold end temperature T_c (°C)	Warm end temperature T_w (°C)	Initial volumetric water content θ_{ini} (%)	Temperature gradient ∇T (°C·cm^{-1})
T1	-6	7	12	1.3
T2	-6	7	24	1.3
T3	-6	7	25	1.3
T4	-11	11	25	2.2

accurately by using the PIV method. At the same time, the cryogenic structure of the segregated ice in the process of segregation frost heave was observed by the image digital experiment system. Finally, the mechanism of segregation frost heave was analysed through the segregation potential principle.

2. Materials and Methods

2.1. Experimental Materials. The test soil samples were taken along the G109 National Highway of Rubber Mountain in Qinghai Province. The basic physical properties of the soil samples are shown in Table 1. The soil samples are silty clay with a low liquid limit. The results of the compaction test show that the maximum dry density of the soil sample is 1.746 g/cm^3, and the optimum water content is 15.2%. The soil particle gradation curve was obtained by the sieving and density meter methods, as shown in Figure 1. The soil freezing characteristic curve (SFCC) of the Qinghai silty clay under different initial volumetric water content was measured by a nuclear magnetic resonance test [22], as shown in Figure 2. The soil-water characteristic curve (SWCC) of the Qinghai silty clay [23] is shown in Figure 3.

2.2. Experimental System. The test system is mainly composed of a temperature control system, sensor system, data acquisition system, PIV system, water replenishment system, and soil column system, as shown in Figure 4.

(1) Temperature control system: the temperatures of the cold end and the warm end of the soil column are controlled by two Arctic series Thermo Scientific A25 low-temperature cool bath circulators to control the circulation of the coolant in the upper and lower thermal plates. The temperature control range of the cool bath is -25~150°C, and the accuracy is 0.01°C. The entire soil column system is placed in a German Votsch C4-600 constant temperature and humidity test box (temperature: -40~80°C; accuracy: 0.1°C; and humidity: 0~100% RH) to ensure the soil column ambient temperature and humidity are constant. The upper and lower thermal plates are all made of stainless steel and are connected to the cool bath through coolant pipes.

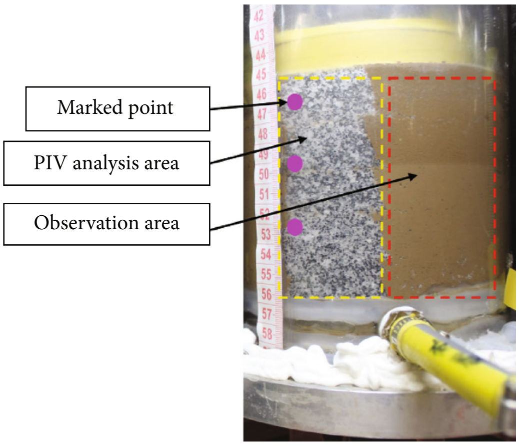

Figure 5: The soil column cylinder drawing.

(2) Sensor system: it is mainly composed of the temperature sensor, the soil moisture sensor, and the displacement sensor. The total height of the soil column is 10 cm, and SUP-WZP PT100 temperature sensors are arranged at intervals of 2 cm along the height of the soil column. A Decagon 5TE [24] soil moisture sensor is arranged at a height of 5 cm of the soil column to measure the average volumetric liquid water content in the entire height of the soil column during freezing (the effective measurement radius of 5TE is 5 cm, the range is 0~50%, and accuracy is ±3%). The top (cold end) of the soil column is installed with a CVB-650F digital displacement meter to measure the total frost heave of the soil column during the freezing process. The measurement range of the digital displacement meter is 0~50.8 mm, the accuracy is ±0.02 mm, and the sampling cycle is 60 seconds. All sensors must be calibrated before use [25].

(3) Data acquisition system: the temperature and moisture sensors are connected to the DataTaker85 data acquisition instrument, connected to the computer through the USB port, and the real-time automatic acquisition of temperature and moisture data is realized based on the SDI-12 communication protocol, and the acquisition interval is set to 60 seconds.

(4) PIV system: the Canon EOS-1300D single-lens reflex camera collects images of the movement of the quartz sand tracer particles during the soil column freezing. A low-temperature LED light is used to provide a stable light field for the camera. The EOS Utility software is used to make the camera remote control and automatic shooting, and the shooting interval is 5 minutes. The geoPIV_RG program is used to obtain the local displacement field of the soil through the captured images [26, 27].

(5) Water supply system: the height of the air inlet of the Marriott bottle is the same as the height of the porous plate at the bottom of the soil column to ensure that the soil column is replenished by capillary action. The constant pressure Marriott bottle provides a constant water head for the soil column and the soil column replenishment amount is calculated by the water level change of the Marriott bottle during freezing.

(6) Soil column cylinder system: the cylinder is made of transparent plexiglass, with an inner diameter of 14 cm and a wall thickness of 1 cm. The lower part of the soil column cylinder is connected to a water tank. The water tank and the soil cylinder are separated by a porous plate which is located on the lower thermal plate. The lower thermal plate, the water tank, and the cylinder are connected by flange plates and screws to form a soil column cylinder system.

2.3. Experimental Method. The frost heave test scheme of the Qinghai silty clay under different initial water contents and temperature gradients under an open system is shown in Table 2. Two different initial volumetric water contents (T1 and T2) and other two different temperature gradients (T3 and T4) were set, respectively. A total of 4 groups of soil column freezing tests were carried out. The dry density and freezing time of each soil column are 1.58 g·cm^{-3} and 144 h, respectively. The temperature gradient refers to the temperature gradient through the entire soil column height.

The dried Qinghai silty clay is pulverized; then, mix the soil according to the initial volumetric moisture content and dry density of the test scheme. The mixed soil is placed in ziplock bags and left for 24 hours to make the water evenly distributed. The diameter of the test soil column is 14 cm and the height is 10 cm, and the compaction degree is controlled by layered compaction. At the same time, the surface texture is constructed with quartz sand particles on one side of the sample cylinder as the PIV analysis area, and the observation area on the other side is used to capture the cryogenic structure of frozen soil during freezing [25], as is shown in Figure 5. A ruler is fixed on one side of the soil column PIV analysis area, and large-diameter quartz sand particles are set as marking points along the soil column heights of 3 cm, 6 cm, and 9 cm. The position of the marked particles relative to the ruler is recorded every 12 hours as the measured value of the soil column local displacement during freezing. After the soil column is completed, install the PT100 temperature sensor and 5TE water sensor according to the design height, wrap the soil column with thermal insulation cotton to reduce the heat loss during freezing, and only the PIV analysis area and the observation area are left for shooting. Connect the sensor, data acquisition instrument DataTaker85, and laptop to debug the sensor system. A layer of plastic film is laid on the top of the soil column to prevent water evaporation and absorption during freezing, and then, the upper thermal plate is installed on it to make it close contact with the top of the soil sample. Install a digital dial indicator on the top of the upper thermal plate, adjust the cold light LED lights in the constant temperature and humidity test box to construct a stable light field for PIV shooting, and erect a Canon EOS-1300D SLR camera in

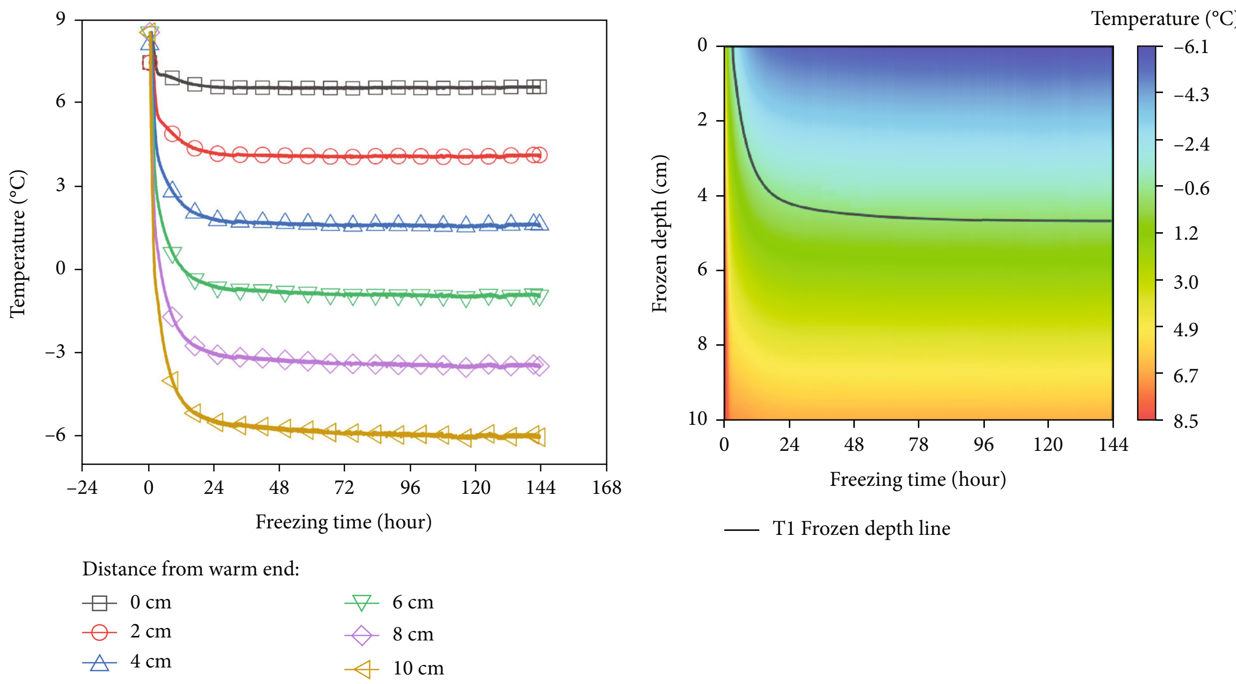

(a) The temperature variation curve of the T1 soil column

(b) The curve of the frozen depth of the T1 soil column

Figure 6: The temperature field variation law of the T1 soil column.

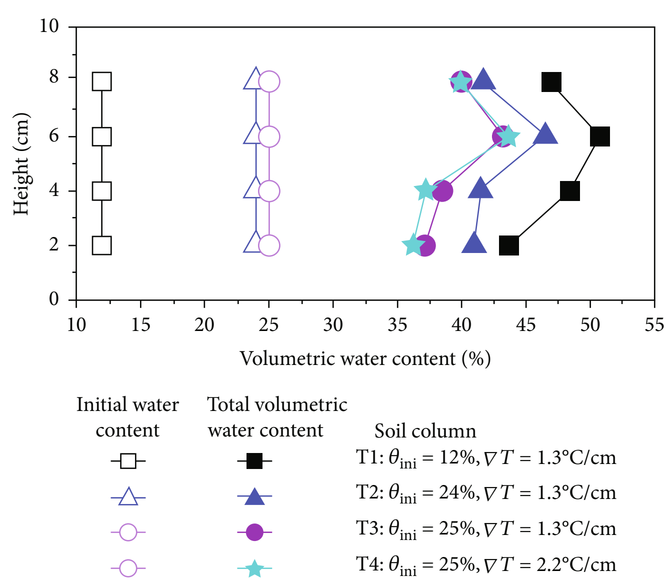

Figure 7: The volumetric water content changes of the soil columns before and after freezing.

front of the soil column. The camera lens must be kept horizontal and perpendicular to the soil column. Connect the camera to the laptop for debugging. The temperature and humidity of the constant temperature and humidity test box are set to 1°C and 0% RH in the whole experiment, respectively. The soil column temperature firstly should be kept constant by the cool bath before freezing. Then it would be started to freeze according to the design temperature boundary conditions. The upper thermal plate is set to the cold end, and the lower thermal plate is set to the warm end. The soil column freezes from top to bottom, and the water migrates from bottom to top. The freezing time is 144 h. After freezing, the soil water content is measured in layers by the drying method.

3. Results

3.1. Law of Temperature Field. After the top and bottom ends of the soil column are loaded with the designed cold end temperature and warm end temperature, respectively,

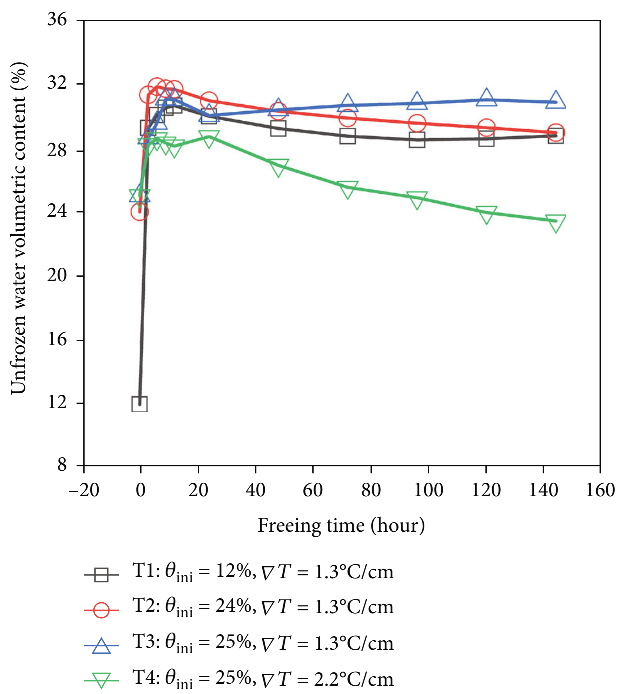

Figure 8: The average unfrozen water volumetric content changes of the soil columns.

the temperature in the soil column decreases rapidly, and physical phenomena such as water migration and ice-water phase transition occur at the same time. Figure 6(a) shows the variation curve of the T1 soil column temperature with freezing time. It can be seen from the figure that the temperature at different heights first decreases rapidly with the freezing time (0-24 h), then decreases slowly (24-75 h), and finally remains stable (75-144 h). The farther from the warm end, the more severe the temperature change, forming a temperature gradient along with the soil column height. The temperature variation laws of other soil columns are similar to this and will not be repeated here.

The initial freezing temperature of the soil is related to the initial water content. According to the research results of Zhou et al. [28], the initial freezing temperature of the soil can be determined from the soil SFCC curve, and then, the frozen depth can be solved by the Lagrange interpolation polynomial [29]. Figure 6(b) is the curve of the frozen depth of the T1 soil column with time. It can be seen from the figure that after the design temperature boundary is applied to the cold and warm ends of the soil column, the freezing front of the T1 soil column gradually moves from the cold end to the warm end of the soil column and finally stabilizes at a certain frozen depth. The entire freezing process can be divided into three stages: fast freezing stage (0~24 h), slow freezing stage (24~75 h), and stable freezing stage (75~144 h). At the fast-freezing stage, the temperature of the soil column decreases sharply, and the freezing front moves rapidly from the cold end to the warm end. After entering the slow freezing stage, the temperature of the soil column changes slowly, and the freezing front still moves downward slightly. At the stable freezing stage, the internal temperature of the soil column is unchanged, the freezing front is also stable at a certain frozen depth, and the frozen depths of other soil columns change similarly. Taking the cold end of the soil column as the zero point of the frozen depth, the frozen depth values of T1~T4 at the end of freezing (144 h) are 4.67 cm, 4.8 cm, 4.9 cm, and 5.0 cm, respectively. It shows that when the temperature gradient is the same, the greater the initial water content, the greater the frozen depth. When the initial water content is the same, the lower the boundary temperature, the greater the frozen depth. Initial water content and boundary temperature are two factors that affect frozen depth.

3.2. Law of Water Field. The moisture of the soil column in the open system will migrate under the action of the matrix potential and the temperature potential. To explore the change in the water content before and after freezing, the drying method is used to measure the water content of the soil column at different heights after freezing. Figure 7 shows the change of volumetric water content before and after the soil column freezing. It can be seen from the figure that the total volumetric water contents of soil columns after freezing are much higher than the initial water contents before freezing, and the water content in the upper frozen zone is greater than that in the lower unfrozen zone, and the total volumetric water contents at the segregation zone (about 6 cm height) reach the maximum. It indicates that the soil column under the open system absorbs a large amount of water from the outside during freezing, and the water from the unfrozen zone migrates to the frozen zone. The total volumetric water content of T1 is greater than that of T2 after freezing, indicating that T1 replenishes more water than T2 throughout the freezing period, which can be verified by the cumulative water replenishment amount of the Marriott bottle below. The total volumetric water content of T3 and T4 frozen zones is basically the same, and the total volumetric water content of T3 is slightly higher than that of T4 in the unfrozen zone.

Figure 8 shows the change in average unfrozen water volumetric content of the soil column with freezing time. It can be seen from the figure that the average unfrozen water volumetric content of the soil column within 6 hours of freezing first increases sharply, then decreases slowly, and remains basically unchanged in the late freezing period, and the average unfrozen water volumetric content of T4 at the freezing later period decreases slightly. This is because the water at the warm end of the soil column under the large temperature potential and matrix potential migrates upwards rapidly within 6 hours after the start of freezing, so the average volumetric content of unfrozen water increases. Then, the freezing front moves down. When the temperature at a certain height is lower than the freezing temperature, the ice-water phase transition will occur here, resulting in a decrease in the unfrozen water content. Finally, when the frozen fringe is stable, the unfrozen water content in the frozen zone remains basically constant, and the water content in the unfrozen zone is replenished and does not also change, so the average unfrozen water volumetric content in the later freezing period remains constant.

The soil column continuously absorbs water during freezing under the open system, and the water level change

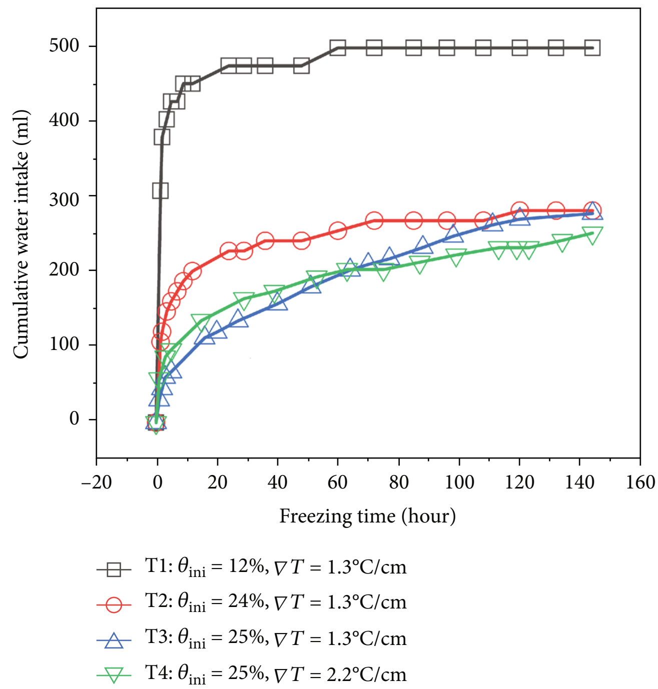

Figure 9: The cumulative water intake changes of the soil columns.

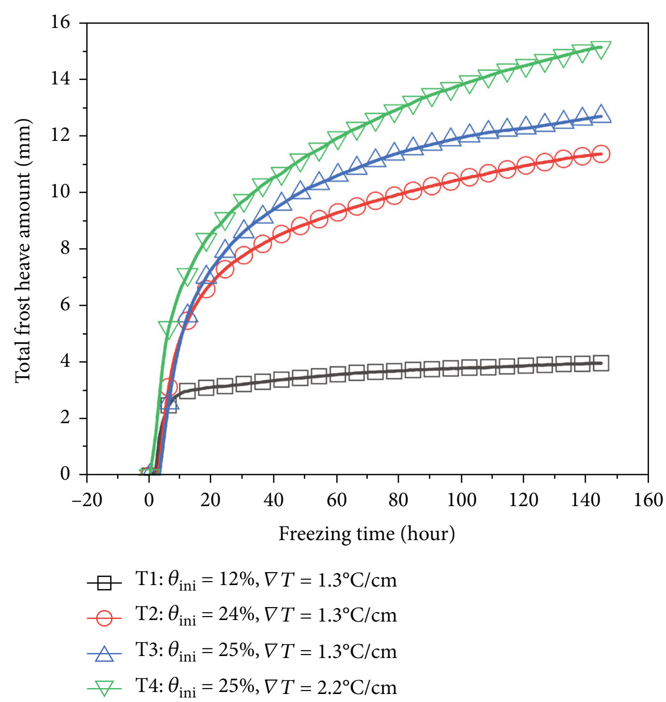

Figure 10: The total frost heave amount changes in the soil columns.

of the Marriott bottle is recorded to calculate the water replenishment amount of the soil column. Figure 9 shows the changes in the cumulative water replenishment of the soil column. It can be seen from the figure that the water replenishment rate is fast and the water replenishment amount is large within 10 hours after the soil column begins to freeze, and then, the water replenishment rate gradually slows down and the water replenishment amount becomes smaller. The T1~T4 soil columns absorb about 498 ml, 282 ml, 278 ml, and 252 ml of water after freezing, respectively. The initial volumetric water content of T1 is much smaller than that of T2, so the soil water potential of T1 is

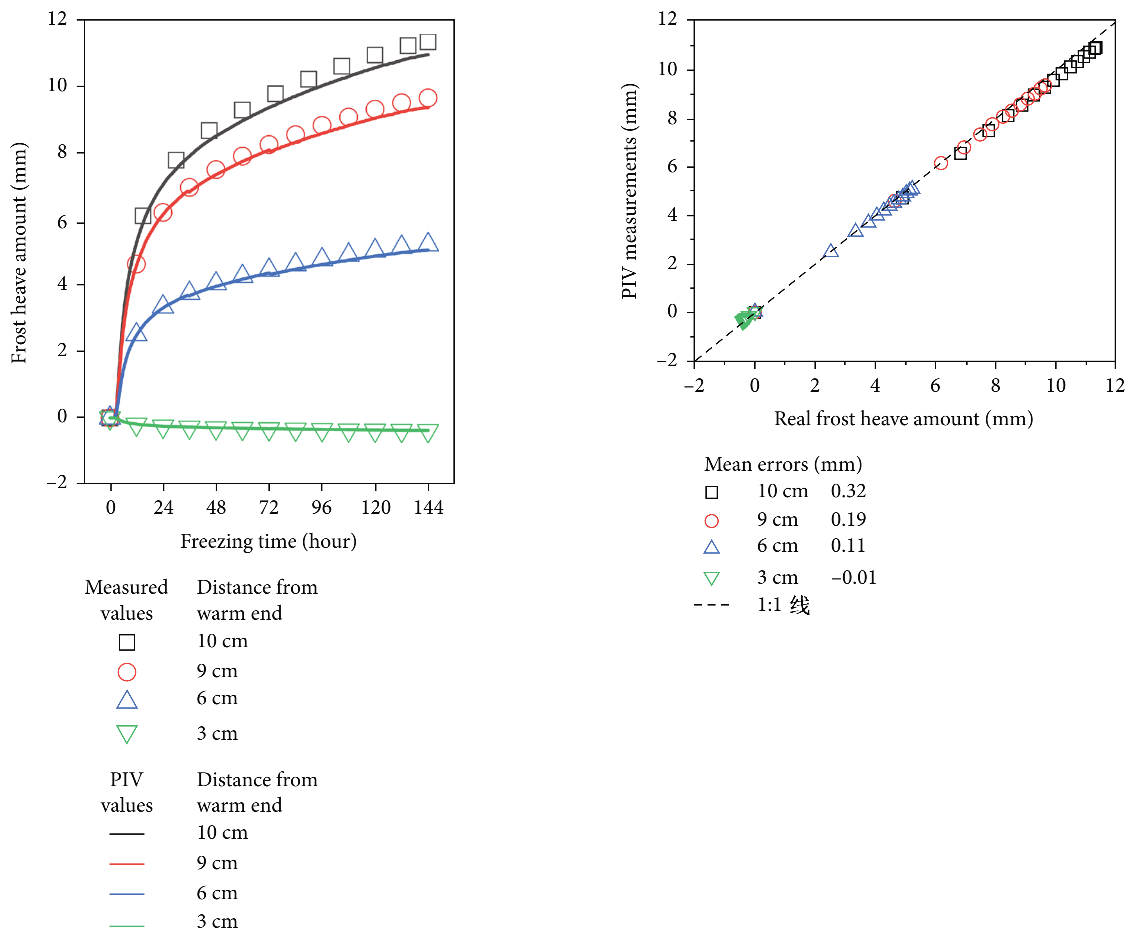

(a) The frost heave amounts at different heights of the T2 soil column (b) The PIV measurement error of the frost heave of the T2 soil column

Figure 11: Frost heave amounts at different heights of the T2 soil column.

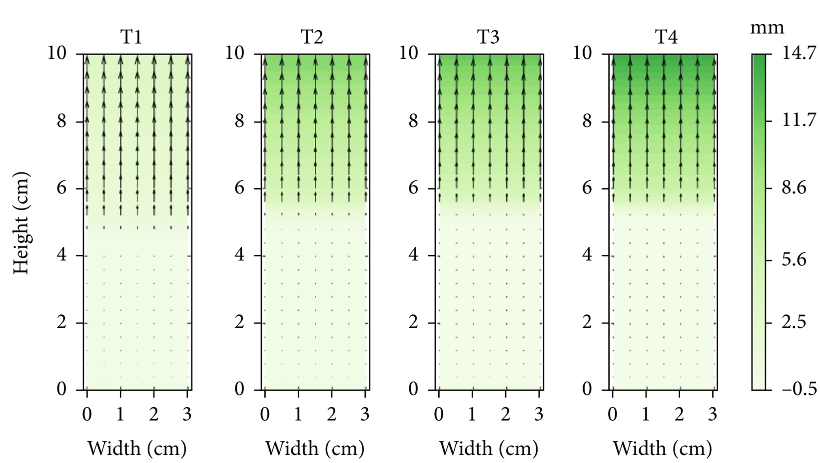

Figure 12: Distribution of PIV measurement value of soil column freezing 144 h displacement.

much greater than that of T2 under the same temperature gradient. Therefore, the accumulated water replenishment amount of T1 is much larger than that of T2 in the first 10 hours of freezing. The water content of soil gradually increases with the freezing time, and the soil water potential gradually decreases. The water replenishment gradually stabilizes in the later period of freezing. It indicates that the soil column with low initial water content has more water replenishment than the soil column with high initial water content under the same temperature gradient. The temperature

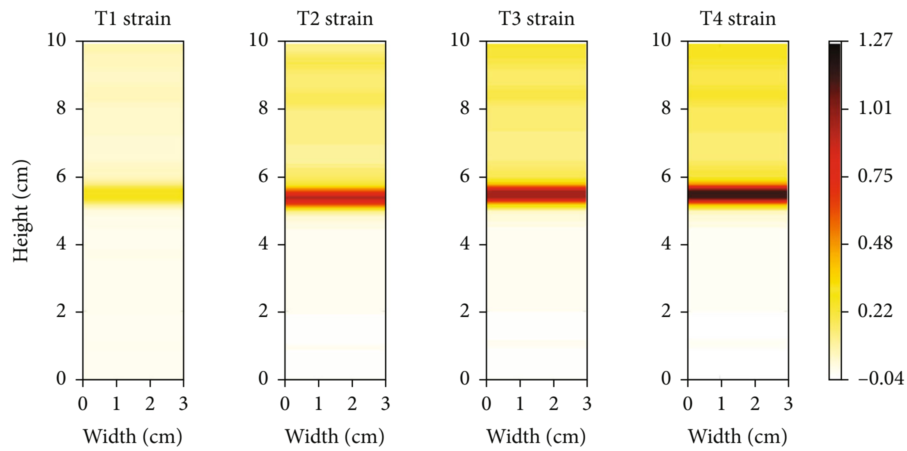

Figure 13: The vertical strain field distributions of the soil columns after freezing 144 h.

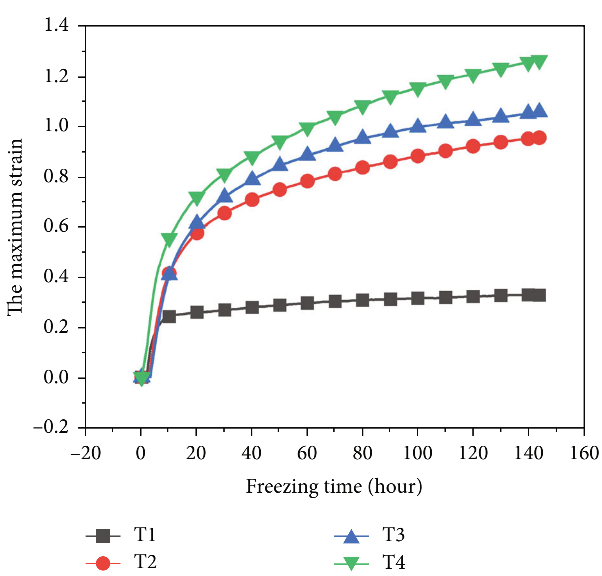

Figure 14: Variation of the maximum strain at the segregation position of the soil column with time.

gradient of T4 is greater than that of T3, and the temperature potential of T4 is greater than that of T3, so the water replenishment amount of T4 is greater than that of T3 in the early stage of freezing. With increasing saturation, the soil water potential of T4 is smaller than that of T3, so the water replenishment amount of T3 is greater than that of T4 in the later stage of freezing.

3.3. Law of Deformation Field. A digital dial indicator was used to record the change of the total frost heave at the cold end of the soil column during the test. Figure 10 shows the total frost heave amount variation at the cold end of the soil column. It can be seen from the figure that the frost heave amount increases sharply within about 10 hours after the start of freezing and then increases slowly. The total frost heave amount of T1~T4 was 3.96 mm, 11.31 mm, 12.67 mm, and 15.10 mm after freezing for 144 h, respectively. The total frost heave amount of T1 is much smaller than that of T2, which indicates that the total frost heave amount of the soil column with large initial water content is larger under the same temperature gradient. The total frost heave amount of T3 is smaller than that of T4, which indicates that the soil column with a large temperature gradient has a larger total frost heave under the same initial water content.

As a noncontact measurement method, PIV has been widely used in small deformation measurement in fluid mechanics and geotechnical engineering [26, 30–32]. PIV is used to measure the local deformation values at different heights of the soil columns. Figure 11(a) shows the PIV values and the measured values of the marked points of frost heave at different heights of the T2 soil column. It can be seen from the figure that the PIV values of frost heave at different heights are slightly smaller than the measured values. This is due to the friction between the tracer particles and the cylinder wall, which causes the displacement of the tracer particles to be smaller than the actual displacement of the soil. The local displacement of the soil column at 3 cm away from the warm end is negative, indicating that the soil is slightly compressive and deformed here. Figure 11(b) shows the PIV measurement error of the frost heave of the T2 soil column. It can be seen from the figure the maximum average error of the PIV measurement values is 0.32 mm, which meets the accuracy requirements. Therefore, the PIV values can be used to estimate the local deformation of the frozen soil.

The PIV method was introduced to measure the displacement distribution of the soil column after freezing for 144 hours, as shown in Figure 12. It can be concluded from the figure that the frost heave deformation occurs in the upper frozen zone of the soil column, and the frost heave amount is positive, and the compression deformation occurs in the lower unfrozen zone, and the compression amount is negative. There is an obvious interface between the frozen zone and the unfrozen zone, which belongs to the frozen fringe, where the ice-water phase transition occurs and new ice lenses are formed to replenish the segregation layer. The maximum frost heave at the top of T1~T4 measured by the PIV method was 3.9 mm, 11.1 mm, 12.4 mm, and 14.7 mm, respectively, and the compression in the unfrozen zone was -0.1 mm, -0.3 mm, -0.4 mm, and -0.5 mm, respectively.

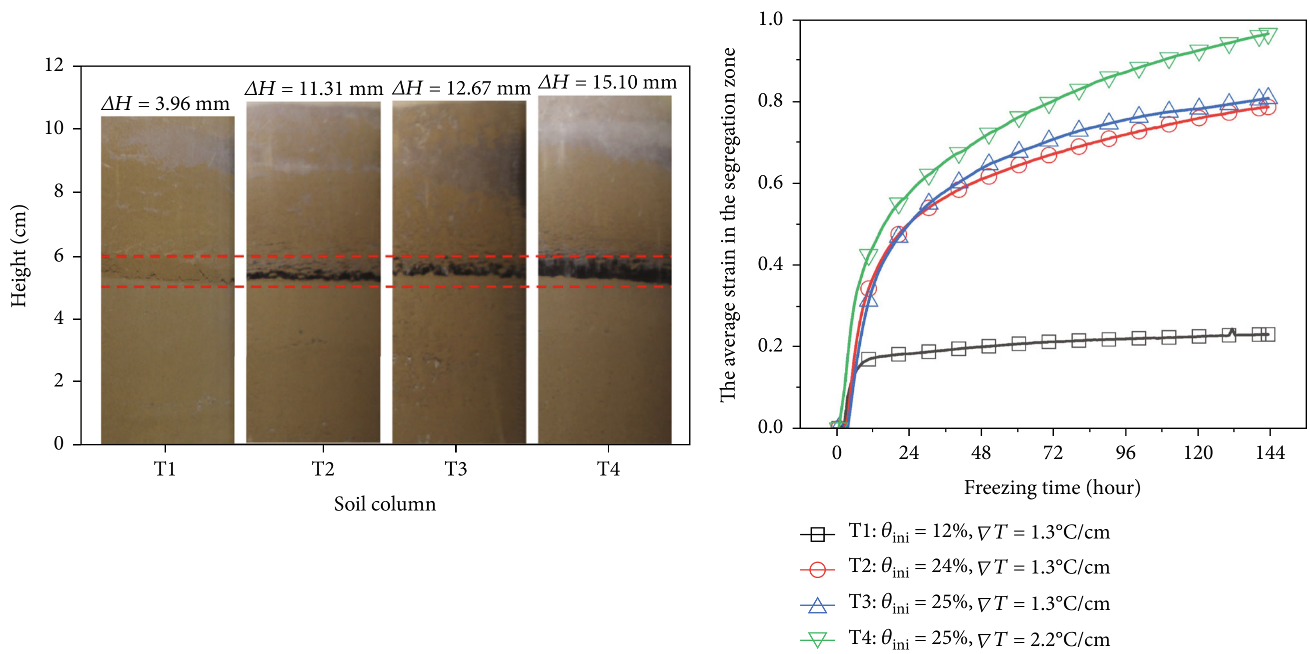

(a) Segregation cracks in soil column after freezing for 144 h

(b) The variation of the average strain in the segregation zone of the soil column

Figure 15: The soil column segregation crack phenomenon.

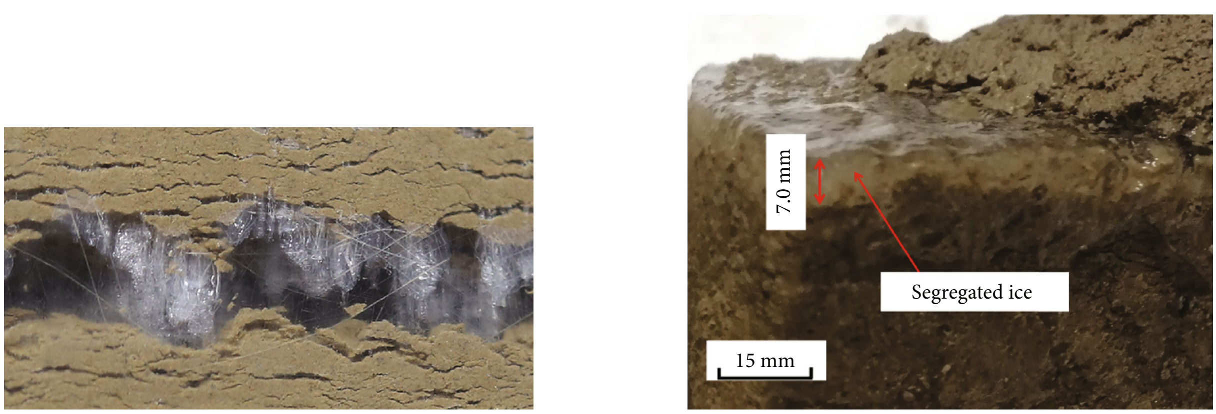

(a) Morphology of segregated ice in segregation cracks in the T4 soil column

(b) The segregated ice layer in the segregation cracks of the T4 soil column

Figure 16: The T4 soil column segregated ice phenomenon.

The strain field reflects the local deformation law of the soil column. According to the geoPIV_RG program, the local displacement value of the soil column during freezing is calculated [27]. The vertical local strain of the soil column is solved by the finite difference method. In order to improve the calculation accuracy, the vertical difference grid side length is 1.0 mm. Figure 13 shows the vertical strain field distribution of the soil column frozen for 144 hours, with positive values representing upward frost heave deformation and negative values representing downward compressive deformation. It can be seen from the figure that the local strain value of the upper frozen zone is positive, indicating that frost heave deformation occurs in the frozen zone, and the local strain value of the lower unfrozen zone is negative, indicating that the unfrozen zone has compressive deformation, and the strain value of the frozen zone is greater than that of the unfrozen zone. The strain value in the segregation zone reaches the maximum positive value, which should be the largest local deformation caused by the precipitation of the segregated ice layer. The maximum strain values of the T1~T4 segregation zone after freezing for 144 h are 0.33, 0.96, 1.06, and 1.27, respectively.

The strain value at the segregation position reflects the size of the local frost heave. The larger the strain value, the greater the amount of frost heave. Figure 14 displays the variation of the maximum strain with time at the segregation position of the soil column. It can be seen from the figure that the increase rate of the maximum strain value of the soil column increases first and then decreases with time. The maximum strain value T4 at the segregation position is

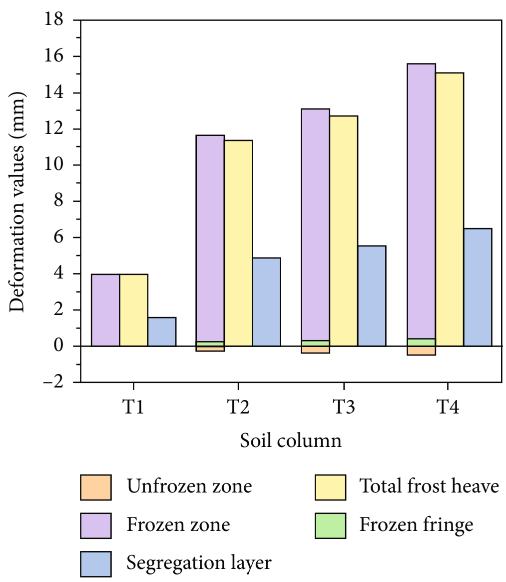

Figure 17: The frost heave deformation distributions of the soil columns.

greater than T3, and T2 is greater than T1. The maximum strain value of the T1 soil column increased very slowly after 10 h of freezing, indicating that the local frost heave also increased less. The maximum strain value of T2~T4 still increases with time after freezing for 10 h, and the amount of segregation frost heave also increases continuously.

4. Discussion for Segregation Frost Heave Law and Mechanism

4.1. Segregation Frost Heave Characteristics. From the soil column image collected by the PIV system during freezing (Figure 15(a)), the horizontal segregation cracks with the layered structure gradually appear in the vertical direction of the soil column under the constant temperature continuous freezing mode. The segregation cracks of T1 are not obvious, T2~T4 have obvious segregation cracks, and the widths are getting larger and larger. The width of segregation cracks increases with the increase of initial water content and temperature gradient. In order to quantitatively describe the time-varying characteristics of the local deformation at the segregation cracks, it is represented by the average strain of the segregation zone (Figure 15(a) the area between the red lines of the soil column). Figure 15(b) shows the variation of the average strain in the segregation zone of the soil columns. It can be seen from the figure that the average strain rate in the segregation zone first increases and then decreases, the average strain value in the segregation zone of the T1 soil column is the smallest, and that of T4 is the largest.

Figure 16(a) shows the local segregated ice morphology in the segregation crack of the T4 soil column captured by the high-definition camera. It can be seen from the figure that the segregated ice lens in the segregation crack presents a needle-column structure from top to bottom, with different sizes, and is incompletely filled with crack pores. Thick layers of segregated ice are partially filled with the segregation crack when disassembling the soil column longitudinally. As shown in Figure 16(b), the thickness of the segregated ice in the segregation cracks of the T4 soil column reaches 7.0 mm. Combined with the total frost heave (15.10 mm) of the T4 soil column, it shows that the appearance of segregated ice is the main reason for the large frost heave amount of the soil column.

4.2. Law of Segregation Frost Heave. The total frost heave of the soil column consists of three parts: the deformation of the frozen zone, the deformation of the frozen fringe, and the deformation of the unfrozen zone [33]. The deformation in the frozen zone is mainly composed of the thickness of the segregated ice in the segregation crack and other migration frost heave and in situ frost heave in the frozen zone. First, the thickness of the frozen fringe and the height of the unfrozen zone are determined according to the positions of the segregation cracks and frozen depth, and then, the local deformation of each zone is calculated from the local strain value of each zone. Figure 17 shows the distribution of frost heave deformation in each zone of the soil column. It can be seen from the figure that there is a large frost heave deformation (positive value) in the frozen zone, a small amount of compression deformation (negative value) in the unfrozen zone, and a small amount of frost heave deformation (positive value) at the frozen fringe. The total frost heave amount and the thickness of the segregation layer of T3 and T2 soil columns are much larger than those of T1, indicating that when the temperature gradient is the same, the higher the initial water content, the greater the total frost heave amount, and the larger the thickness of the segregation layer. The total frost heave amount and the thickness of the segregation layer of the T4 soil column are greater than those of T3, indicating that when the initial water content is the same, the higher the temperature gradient, the greater the total frost heave amount, and the larger the thickness of the segregation layer. Initial water content and temperature gradient are two important factors affecting soil frost heave under an open system. Measures such as antiseepage can be taken to reduce the initial soil water content and set some thermal insulation measures to reduce the temperature gradient inside the soil to weaken the frost heave disease of geotechnical engineering in cold regions. The thicknesses of the segregated ice of the T1~T4 soil column are 40.8%, 43.1%, 43.2%, and 44.4% of the total frost heave amount, respectively. It can be concluded that segregation frost heave caused by water migration is the main factor for soil column frost heave deformation.

4.3. Segregation Frost Heave Mechanism. The frost heave of the soil column under an open system is a complex coupled process of hydrothermal and mechanical [34–36]. As shown in Figure 18, when the temperature T_c and T_w are applied to the cold end and the warm end of the soil column, a temperature gradient will be formed in the soil column. And the water in the soil column will migrate from the warm end to the cold end under the action of the matric potential and temperature potential. A freezing front appears when

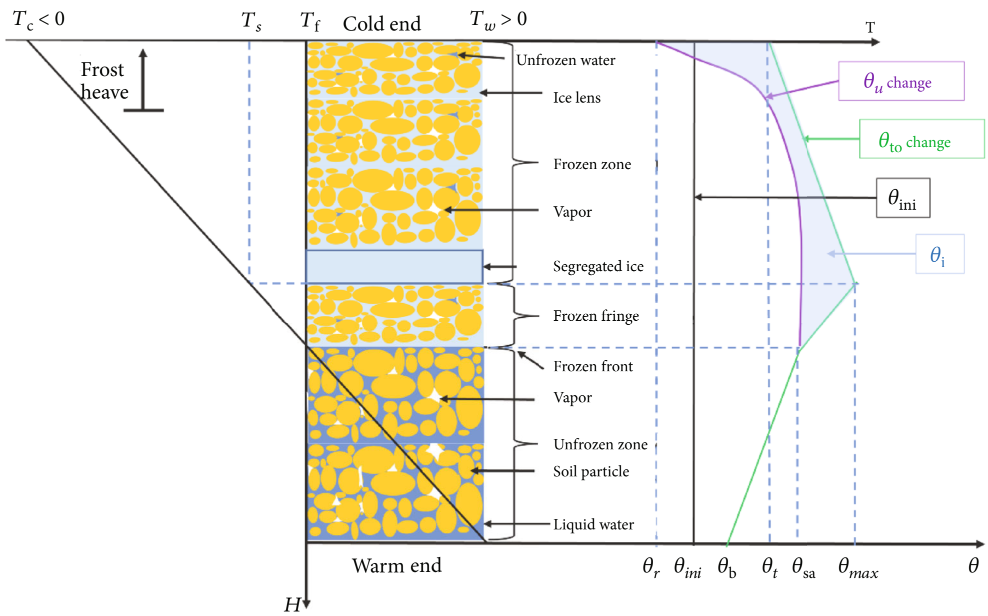

Figure 18: Schematic of soil column segregation frost heave.

the temperature at a certain height of the soil column is equal to the freezing temperature T_f. In addition, the frozen fringe also begins to form, where water migration and ice-water phase transition occur. As the temperature continues to decrease, the freezing front and frozen fringe continue to move to the warm end, and the frozen zone continues to expand. The liquid water in the frozen zone gradually condenses into ice crystals and fills the pores until it is equal to the residual unfrozen water content. The water in the Marriott bottle continuously replenishes the soil column in the form of capillary water under the matric potential. After the soil temperature stabilizes, the freezing front stops moving, and the water continuously moves to the warm end of the segregated ice and undergoes a phase change, and the segregated ice gradually thickens and eventually forms a thick layer of segregated ice above the frozen fringe.

The initial water content of the soil column before freezing is θ_{ini}. Under the action of water replenishment, the liquid water content θ_u of the soil column increases sharply first. When the liquid water content θ_u increases to θ_t at the cold end, the liquid water content θ_u near the frozen fringe first reaches the saturated water content $\theta_{sa.}$ The water in the unfrozen zone continuously migrates to the frozen fringe and the segregated layer with freezing. The liquid water in the frozen zone begins to form pore ice and segregated ice. Then, the liquid water content θ_u decreases, the ice content θ_i begins to increase, and θ_u finally is equal to the residual unfrozen water content θ_r in the frozen zone. The ice content θ_i at the segregation layer reaches the maximum value. The total water content θ_{to} at the cold end of the frozen zone is θ_t, the total water content at the segregation layer θ_{to} reaches the maximum value θ_{max}, and the total water content θ_{to} in the warm end of the unfrozen zone is θ_b.

There is water and heat transfer inside the soil column during freezing, and the frozen fringe contains complex physical processes such as water migration, ice-water phase transition, and ice lens formation. According to the theory of segregation frost heave potential [7], the frost heave amount is mainly controlled by the thickness of the segregated ice. When the soil saturation is low, the presence of pore gas in the soil makes it difficult for ice crystals to form and be observed, such as the T1 soil column, which has no obvious segregation crack, and the segregated ice content is also very small, so the frost heave amount is small. When the soil saturation is high and there is some closed pore gas, the capillary water is more likely to migrate to the frozen fringe under the capillary action of the soil pores to form segregated ice, and soil column has obvious segregation cracks and a large frost heave amount, such as T2~T4 soil columns.

5. Conclusions

Based on the self-developed PIV soil column frost heave test system, the influence of different initial water contents and temperature gradients on the segregation frost heave of the soil column was explored, and the following conclusions were drawn:

(1) The soil column of silty clay undergoes obvious heat and water migration during freezing under the open system. The total volumetric water content after freezing is much greater than the initial water content before freezing, and the total volumetric water content in the segregation zone reaches the maximum value. The average unfrozen water content first increases sharply with time, then decreases slowly, and remains unchanged after the soil temperature stabilizes.

(2) Large frost heave deformation occurs in the frozen zone, small compression de-formation occurs in the unfrozen zone, and a small amount of frost heave deformation occurs in the frozen fringe. There are

obvious layered segregation cracks at a certain height of the soil column, and unsaturated needle-cylindrical ice lenses are filled in the segregation cracks forming a local thick layer of segregated ice. The thickness of the segregated ice is about 43% of the total frost heave of the soil column.

(3) Under the same temperature gradient conditions, the soil column with the low initial water content has a smaller freezing depth, larger total volumetric water content, more water intake, smaller segregation ice thickness, and less total frost heave amount than that of the soil column with the high initial water content. Under the same initial water content conditions, the soil column with a large temperature gradient has a greater freezing depth, consistent total volumetric water content, larger segregation ice thickness, and greater total frost heave amount than that of the soil column with a small temperature gradient.

Nomenclature

d: Diameter of soil column (cm)
H: Height of soil column (cm)
W: Width of PIV analyse area (cm)
ΔH: Total frost heave mount (mm)
T: Temperature (°C)
t: Freezing time (h).

Greek Symbols

ρ: Density (g/cm^3)
θ: Volumetric water content (cm^3/cm^3)
ψ: Matrix suction (KPa)
ω: Mass water content.

Mathematics Symbol

∇: Differential operator.

Subscripts

c: Cold end
d: Drying state
w: Warm end
s: Position of segregated ice
f: Frozen depth position
ini: Initial state
i: Ice
to: Total water amount
u: Unfrozen water
r: Residual liquid water
b: Warm end of soil column
t: Cold end of soil column
sa: Saturation water content
max: Maximum value.

Data Availability

The data used to support the findings of this study are available from the corresponding author upon request.

Conflicts of Interest

The authors declare that they have no known competing financial interests or personal relationships that could have appeared to influence the work reported in this paper.

Acknowledgments

This research was supported by the Fundamental Research Funds for the Central Universities (No. 2020YJS115), the National Natural Science Foundation of China (No. 51979002), and the Beijing Natural Science Foundation (No. 8192034).

References

[1] Q. Miao, F. Niu, Z. Lin, and J. Luo, “Progress and prospects of research on frost heave of high-speed railway subgrade in seasonally frozen regions,” *Journal of Glaciology and Geocryology*, vol. 41, no. 3, pp. 669–679, 2019.

[2] H. Zhao, Q. Wu, Z. Zhang, and Y. Hou, “Assessment of cooling effect of the crushed rock embankment based on catastrophe progression method,” *Chinese Journal of Rock Mechanics and Engineering*, vol. 38, no. 8, pp. 1686–1695, 2019.

[3] T. Hu, T. Wang, J. Liu, and J. Chang, “Design and experiment on a solar heat-supplying tube against frost damage of embankment in cold regions,” *China Civil Engineering Journal*, vol. 52, pp. 44–52, 2019.

[4] S. Akagawa, M. Hori, and J. Sugawara, “Frost heaving in ballast railway tracks,” *Procedia Engineering*, vol. 189, pp. 547–553, 2017.

[5] Q. Zhang, Q. Wang, J. Fang et al., “Study of the characteristics mechanical damage and constitutive model of crushed-rocks from high-grade highway in permafrost region,” *Geofluids*, vol. 2022, Article ID 7439860, 17 pages, 2022.

[6] P. He, W. Ma, Y. Mu, J. Dong, and Y. Huang, “Elastic foundation beam model for frost heave damage of trapezoidal canal lining considering frost heave force and adfreeze force,” *Journal of Central South University (Science and Technology)*, vol. 52, no. 11, pp. 4148–4157, 2021.

[7] F. Liu, W. Ma, Z. Zhou, S. Zhang, Y. Mu, and P. He, “Deformation and stress variation characteristics of canal foundation soils under freeze-thaw cycles,” *Journal of Glaciology and Geocryology*, vol. 43, no. 2, pp. 523–534, 2021.

[8] H. He, J. Teng, S. Zhang, and D. Sheng, “Rationality of frost susceptibility of soils,” *Chinese Journal of Geotechnical Engineering*, vol. 44, no. 2, pp. 224–234, 2022.

[9] J. M. Konrad and N. R. Morgenstern, “A mechanistic theory of ice lens formation in fine-grained soils,” *Canadian Geotechnical Journal*, vol. 17, no. 4, pp. 473–486, 1980.

[10] X. Xu, L. Zhang, and J. Wang, “Essential types of heave development for soil freezing,” *Journal of Glaciology and Geocryology*, vol. 4, pp. 301–307, 1994.

[11] G. Zhao, X. Tao, and B. Liu, “Experimental study on water migration in undisturbed soil during freezing and thawing process,” *Chinese Journal of Geotechnical Engineering*, vol. 31, no. 12, pp. 1952–1957, 2009.

[12] H. Wei, J. Zhou, C. Wei, and P. Chen, “Experimental study of water migration in saturated freezing silty soil,” *Rock and Soil Mechanics*, vol. 37, no. 9, p. 2547-2552+2560, 2016.

[13] Z. Liu, J. Liu, X. Li, and J. Fang, "Experimental study on freezing point and deformation characteristics of unsaturated silty clay subjected to freeze-thaw cycles," *Chinese Journal of Geotechnical Engineering*, vol. 39, no. 8, pp. 1381–1387, 2017.

[14] Y. Wang, D. Wang, W. Ma, Y. Mu, H. Guan, and T. Gu, "Experimental study of development of cryostructure and frost heave of the Qinghai-Tibet silty clay under one-dimensional freezing," *Rock and Soil Mechanics*, vol. 37, no. 5, pp. 1333–1342, 2016.

[15] W. Huang, *Element Test Study on the Freezing Deformation Characteristics of Unsaturated Soil*, Beijing Jiaotong University, Beijing, 2021.

[16] X. Ren, Q. Yu, J. Wang, D. Zhang, Z. Zhang, and X. Wang, "Experimental study on the characteristics of cryostructure and frost heave of clay under one-dimensional freeze-thaw," *Journal of Hydraulic Engineering*, vol. 52, no. 1, pp. 81–92, 2021.

[17] Z. Xiao, Y. Lai, and Z. You, "Water and salt migration and deformation mechanism of sodium chloride soil during unidirectional freezing process," *Chinese Journal of Geotechnical Engineering*, vol. 39, no. 11, pp. 1992–2001, 2017.

[18] G. H. Go, J. Lee, H. S. Shin, B. H. Ryu, H. W. Jin, and D. W. Kim, "Evaluation of one-dimensional freezing behavior for ice-rich sandy soil," *International Journal of Heat and Mass Transfer*, vol. 130, pp. 960–967, 2019.

[19] H. W. Jin, J. Lee, B. H. Ryu, and S. Akagawa, "Simple frost heave testing method using a temperature-controllable cell," *Cold Regions Science and Technology*, vol. 157, pp. 119–132, 2019.

[20] Y. Wang, D. Wang, W. Ma, Z. Wen, X. Xu, and H. Du, "Development and application of frost heaving experimental system based on the digital image processing," *Journal of Glaciology and Geocryology*, vol. 39, no. 5, pp. 1047–1056, 2017.

[21] Y. Zhou and J. Zhang, "A novel visualization apparatus for freezing soils and its application in freezing-thawing test," *Chinese Journal of Rock Mechanics and Engineering*, vol. 39, no. 8, pp. 1671–1681, 2020.

[22] M. Wang, X. Li, and X. Xu, "An implicit heat-pulse-probe method for measuring the soil ice content," *Applied Thermal Engineering*, vol. 196, article 117186, 2021.

[23] X. Li, A. Liu, L. Liu, Y. Liu, and Y. Wu, "A rapid method for determining the soil-water characteristic curves in the full suction range," *Rock and Soil Mechanics*, vol. 43, no. 2, pp. 299–306, 2022.

[24] Decagon, *5TE_Manual*http://www.misure.net/sites/default/files/pdf/20435_5TE_Manual_Web.pdf, 2018.

[25] M. Wang, X. Li, Z. Liu, J. Liu, and D. Chang, "Application of PIV technique in model test of frost heave of unsaturated soil," *Journal of Cold Regions Engineering*, vol. 34, no. 3, p. 04020014, 2020.

[26] S. A. Stanier, J. Blaber, W. A. Take, and D. J. C. G. J. White, "Improved image-based deformation measurement for geotechnical applications," *Canadian Geotechnical Journal*, vol. 53, no. 5, pp. 727–739, 2016.

[27] C. Gallage and C. P. Gunasekara Jayalath, "Use of particle image velocimetry (PIV) technique to measure strains in geogrids," *Proceedings of the 7th International Symposium on Deformation Characteristics of Geomaterials (IS-Glasgow 2019)*, vol. 92, 2019, pp. 1–6, EDP Sciences, 2019.

[28] J. Zhou, X. Meng, C. Wei, and W. Pei, "Unified soil freezing characteristic for variably-saturated saline soils," *Water Resources Research*, vol. 56, no. 7, p. e2019WR026648, 2020.

[29] T. Wang, H. Ma, J. Liu, Q. Luo, Q. Wang, and Y. Zhan, "Assessing frost heave susceptibility of gravelly soils based on multivariate adaptive regression splines model," *Cold Regions Science and Technology*, vol. 181, article 103182, 2021.

[30] Z. Liu, J. Liu, X. Li, T. Hu, and J. Fang, "Application of PIV in model tests on frozen unsaturated soils and grayscale correlation analysis," *Chinese Journal of Geotechnical Engineering*, vol. 40, no. 2, pp. 313–320, 2018.

[31] T. Jiang, T. Zhai, J. Zhang et al., "Diametric splitting tests on loess based on particle image velocimetry technique," *Rock and Soil Mechanics*, vol. 42, no. 8, p. 2120-2126+2140, 2021.

[32] T. Jiang, T. Zhai, J. Zhang et al., "Diametric splitting tests on loess based on PIV technique," *Rock and Soil Mechanics*, vol. 8, pp. 1–8, 2021.

[33] X. Xu, J. Wang, and L. Zhang, *Frozen Soil Physics*, Science Press, Beijing, 2010.

[34] S. S. Peppin and R. W. Style, "The physics of frost heave and ice-lens growth," *Vadose Zone Journal*, vol. 12, no. 1, pp. 1–12, 2013.

[35] X. Xu and Y. Deng, *Experimental Study on Water Migration in Freezing and Frozen Soils*, Science Press, Beijing, 1991.

[36] H. R. Jacobs and F. M. Perkins, "Determination of thermal conductivity in freezing moist soils," *Experimental Thermal and Fluid Science*, vol. 3, no. 4, pp. 355–361, 1990.